
Application of coarse-grained diamond grinding wheels for precision grinding of glass ceramics

Barnabás Adam^{1,2}, Kai Rickens¹, Olthmann Riemer^{1,2}, Carsten Heinzel^{1,2}

¹ Leibniz Institut für Werkstofforientierte Technologien IWT, Laboratory for Precision Machining LFM, Badgasteiner Straße 2, 28359 Bremen, Germany

² MAPEX Center for Materials and Processes, University of Bremen, Germany

adam@iwt.uni-bremen.de

Abstract

Precision grinding enables the economic machining of brittle-hard materials. High surface qualities, low subsurface damage and tight tolerances can be achieved due to ductile material removal. Fine-grained grinding tools with soft bonds are usually applied for precision grinding of brittle materials, as they reduce the maximum uncut chip thickness and support ductile material removal. But, one disadvantage is their vulnerability to wear, which reduces efficiency and can lead to form errors. Coarse-grained diamond grinding wheels can address these disadvantages. However, the use and applicability of these grinding wheels has not yet been conclusively investigated.

In this research, the applicability of diamond grinding wheels with grain sizes of D301, D601 and D851 for precision grinding of grooves in a glass ceramic is investigated. The topographies of the grinding wheels are characterised and the diamond grains expected to be engaged with the workpiece material are determined. Grinding experiments with in-process force measurement were carried out to investigate the influence of cutting speed on the material removal mechanism and to calculate the loads in machining.

Results show that ductile material removal is possible with coarse-grained diamond grinding wheels. Surfaces with roughness of about 60 nm to 175 nm could be generated. Higher cutting speeds could achieve lower surface roughness. The correlation between a higher cutting speed and lower resulting normal forces cannot be shown consistently. Furthermore, calculation of the load stresses in machining by measuring forces and by characterising the grinding wheel topography is possible.

Precision grinding, coarse-grained diamond grinding wheels, surface roughness, material removal mechanism

1. Introduction

Economic machining of optical and precision components from brittle-hard materials is achieved with precision grinding. A ductile material removal mechanism enables the generation of high surface qualities, low subsurface damage and tight tolerances [1, 2].

Usually fine-grained and soft bonded grinding tools are used for precision machining. This is due to the advantage that small grain sizes reduce the maximum uncut chip thickness and thus, support a ductile material removal mechanism. However, one of the main disadvantages of fine-grained soft-bonded grinding tools is their tendency to wear, which reduces overall efficiency and can lead to form errors. [1,3,4].

A possible solution can be coarse-grained grinding wheels which are less vulnerable to wear due to their grain size and hard bonds. But it is challenging to design grinding processes with coarse-grained grinding wheels in precision grinding, as existing calculation formulas, such as the maximum uncut chip thickness according to Malkin [4] and the critical uncut chip thickness according to Bifano [5], can only be applied to a limited extent [1,3,6].

Based on Malkin's formula, the density of active cutting edges and grain size have an effect on the maximum uncut chip thickness $h_{cu,max}$ and thus, on the dominant material removal mechanism [4]. For precision grinding, fine-grain wheels are generally used for this reason. They have a high grain density i.e. a high number of active cutting edges C_{kin} and small grain

diameters which reduces the maximum uncut chip thickness and thus, supports a ductile material removal mechanism. In addition, the stochastic distribution of the grains supports the applicability of the calculation formula described. For example, deviations of individual grains from the average grain shape used in the formula are not significant for high grain densities. It is questionable, however, whether this is the case for coarse grit diamond grinding wheels. Coarse grinding wheels have a low grain density compared to fine grinding wheels. The stochastic distribution of the abrasive grains is limited. This has already been shown in earlier research work. In addition, it could also be shown that precision grinding with coarse-grained grinding wheels is possible and a ductile material removal mechanism can also be achieved [6,7]. Based on these results, a more detailed investigation of the application of a coarse-grained grinding wheel is to be carried out, focussing on the characteristics of the grinding wheel topography and detecting individual grain engagement in the force measurement. The aim is to gain a better understanding of the material removal mechanism.

2. Materials and methods

In this research, characterization of grinding wheel topographies and grinding experiments are carried out for machining of the glass ceramic ZERODUR with diamond grinding wheels of grain sizes D301, D601 and D851 at varying cutting speed v_c . The objective was to investigate to which extent ductile material removal can be realized with the coarse-grained

diamond grinding wheels and whether individual grain engagements are recognizable in the force measurement in order to calculate loads in the contact area and to gain a better understanding of the process and material removal mechanism.

The grinding wheels applied are sintered tools with blocky diamond grains, which were manufactured using reverse plating. According to the manufacturer, the envelope curve deviation is therefore less than $2\ \mu\text{m}$. Each wheel has a radius of 40 mm and a spherical segment shape, which radius is also 40 mm.

The grinding wheel topography is characterised using a Bruker Alicona InfiniteFocus G5 tool measuring system and a MATLAB script, which determines the active grains and their contact surfaces based on the depth of cut a_e . The entire grinding wheel circumference is measured using 5x magnification.

Plunge grinding experiments were performed on a Cranfield Precision TTG 350 Twin Turret Generator. The experimental setup is shown in Figure 1. A workpiece with a diameter of 50 mm and a thickness of 8 mm is glued on a workpiece holder, which is mounted on a dynamometer type 9119AA1 from Kistler. The dynamometer is clamped in the main spindle. The tool is located on the vertical grinding spindle. The process forces are measured at a measuring frequency of 100 kHz using a MATLAB script.

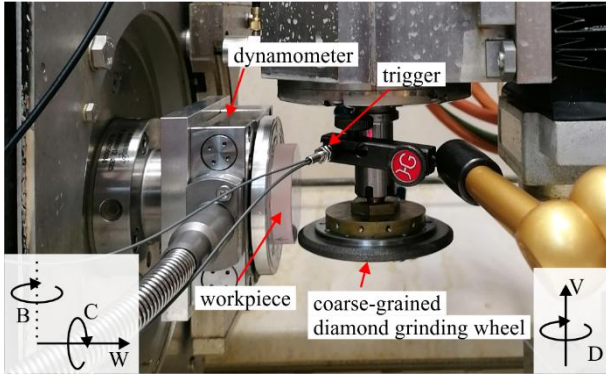


Figure 1. Experimental setup

A touching procedure is applied before each experiment in the center of the groove to be machined. 10 mm long grooves are ground with a constant depth of cut a_e of $1.5\ \mu\text{m}$ and a constant feed rate of v_w of 10 mm/min. The low depth of cut was chosen to minimise the number of grains in contact, and thus simplify their detection. The cutting speed v_c is varied at 30, 45 and 60 m/s and the grain size of the grinding wheels at D301, D601 and D851. The parameters are listed in Table 1. The individual parameter combinations are each carried out three times in order to obtain a sufficient number of experiments for the evaluation and to be able to identify outliers.

Table 1 Experimental parameters

Machine: Cranfield Precision TTG 350 Twin Turret Generator
Material: ZERODUR
Process: Plunge grinding
Parameters:
$v_w = 10\ \text{mm/min}$
$v_c = 30 ; 60\ \text{m/s}$
$a_e = 1.5\ \mu\text{m}$
Grinding fluid: none (dry machining)
Tools: Coarse-grained diamond grinding wheel, D301, D601, D851 (reverse plated)

Machining without grinding fluid had to be selected to enable the use of a trigger. This uses a laser to record the individual

revolutions of the grinding wheel and synchronises them with the force measurement. This allows the forces to be attributed to the individual revolutions of the grinding wheel and thus, also to the engagement of the grains of the grinding wheel.

The generated surface topography is measured using white light interferometry (WLI). A 50x magnification and a measuring area of $0.34\ \text{mm} \times 0.34\ \text{mm}$ is applied for topography characterization. Furthermore a cut-off λ_c of 0.08 mm is applied. Each groove was measured three times.

3. Results and discussion

3.1. Grinding wheel topography analysis

Figure 2 shows an example of the measured grinding wheel topography of the D301 grinding wheel. The active grains are marked in the figure. According to the MATLAB analysis, these should come into contact with the workpiece. It can be seen that according to the analysis, only three grains are active and will remove material. This observation was made with all the grinding wheels considered and also occurred with repeated measurements. Nevertheless, it is likely that the clamping of the grinding wheels during measurement has an influence on the measurement result and the reflectivity of the diamond grains can also lead to measurement artefacts and missing measuring points, which can influence the evaluation.

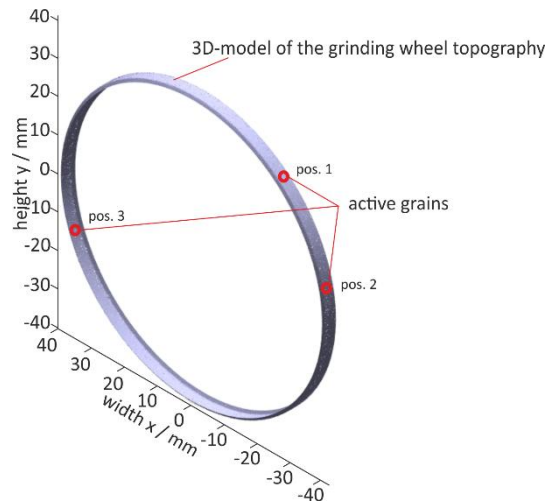


Figure 2. 3D-model of the surface topography of the D301 grinding wheel with marked active grain distribution

Table 2 shows the evaluation of the active grains indicating the number of active grains per grinding wheel and the estimated grain area in contact based on the positions. The contact surfaces are divided into the normal and tangential directions which is analogous to the categorisation of the process forces into normal and tangential force as shown in Figure 3. A tilt of the surfaces of up to 10° is also regarded as a surface in normal direction.

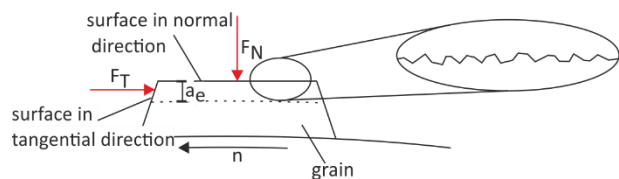


Figure 3. Schematic of a coarse grain and categorisation of the grain surface directions

Table 2 also shows that all grinding wheels have three active grains. The low number of active grains is not surprising, as the depth of cut was below the tolerance of the envelope curve of the grains. Most surfaces are recognised as surfaces in tangential direction which is unexpected, since the normal surfaces should be larger than the surfaces in the tangential direction. This may be justified by several reasons. E.g. on the one hand, missing measuring points can influence the evaluation. Furthermore, it is possible that the grains are not completely flattened, as shown in Figure 3, and therefore the normal surfaces are also evaluated as surfaces in the tangential direction. This is particularly evident when taking a closer look at the individual grains. Therefore, the calculated areas in the tangential direction are added to the areas in the normal direction in the further analysis.

Table 2 Contact surfaces of the active grains

	Position	Surfaces in normal direction / μm^2	Surfaces in tangential direction / μm^2
D301	1	$\ll 1$	145
	2	$\ll 1$	59
	3	$\ll 1$	37
D601	1	$\ll 1$	66
	2	$\ll 1$	82
	3	$\ll 1$	27
D851	1	$\ll 1$	62
	2	$\ll 1$	26
	3	1	54

3.2. Surface topography

Figure 4 shows the mean square height S_q of the measured grooves with error bars representing the absolute variation, i.e. the minimum and maximum measured values. No results are shown for grinding wheels D601 and D851 with a cutting speed of $v_c = 60$ m/s as these experiments had to be aborted due to high forces.

Most measurements resulted in S_q values in the range of 60 nm to 175 nm. It can be determined that the cutting speed v_c has no clear influence on the generated surface roughness. According to Malkin's formula for calculating the maximum uncut chip thickness [5], a higher cutting speed should lead to a lower maximum uncut chip thickness and thus, result in lower generated roughness. This correlation cannot be observed with the coarse-grained diamond grinding wheels investigated here.

An influence of the grain size can be observed to a limited extent. For example, lower surface roughness can be generated with grain sizes D301 and D851 than with grain size D601.

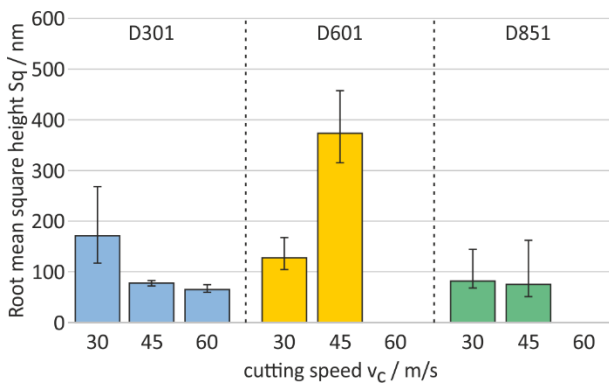


Figure 4. Root mean square height S_q of the experiments

The areal material ratio S_{mr} can provide an indication of the prevailing material separation mechanism. This indicates the

contact ratio at a height value c , which was $1 \mu\text{m}$ for the evaluation. A comparison of the S_{mr} value with the qualitative observation of the surfaces produced has revealed a correlation. A S_{mr} value above 70% with a low variation indicates a ductile material removal mechanism. If S_{mr} is below 30% and has a low variation, brittle material removal is predominant. The ductile-brittle range lies between 30% and 70%. If there is a high absolute variation in the S_{mr} value, this indicates a ductile material removal mechanism with brittle components in individual measurements. If the absolute variation ranges from 0% to 100%, there are areas in the measurements under consideration that exclusively show a ductile material removal mechanism and also exclusively a brittle material removal mechanism, leading to an average in the ductile-brittle range.

Figure 5 shows the S_{mr} value of the experiments carried out. As described above, ZERODUR can usually only be categorised as brittle or ductile-brittle material removal. The parameter combinations D301 and $v_c = 45$ m/s and D851 and $v_c = 45$ m/s are exceptions. Here, ductile material removal could be realised throughout. This observation is supported by the low surface roughness S_q with the parameter combinations.

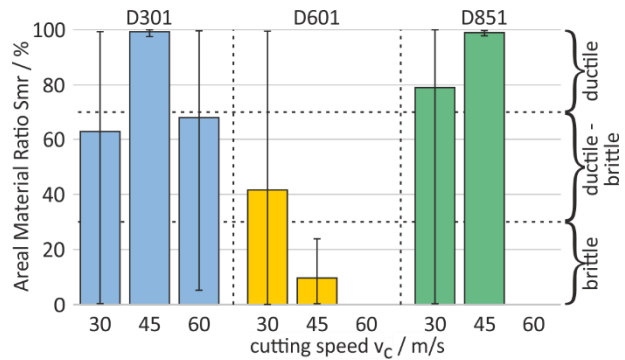


Figure 5. Areal Material Ratio S_{mr} of the experiments

3.3. Process forces

The force measurements are analysed using a MATLAB script. For this purpose, an offset and a drift correction are performed first. The force measurements are then divided into individual revolutions of the grinding wheel using the trigger signal and averaged to obtain an average force curve for one revolution. This is shown exemplary in Figure 6. The error bars represent the variation within the force measurement. Figure 6 also shows that there are two high peaks in one revolution. These peaks are interpreted as grain engagements. Furthermore, a smaller peak can be seen between the two peaks, which can also be interpreted as the engagement of a grain corresponding to the number of active grains measured.

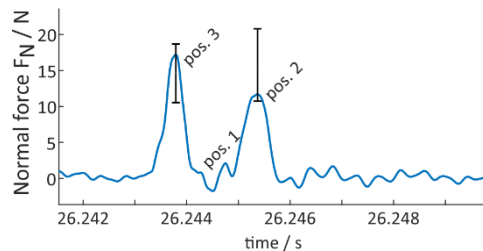


Figure 6. Averaged normal forces of all revolutions and positions of active grains of the D301 grinding wheel machining with $v_c = 30$ m/s and $a_e = 1.5 \mu\text{m}$

However, the above observations do not apply to all force measurement data. For example, significantly more peaks were identified on grinding wheel D851 than active grains were

determined. This is shown as exemplary in Figure 7. A total of nine peaks can be identified here, which indicates grain engagement. This suggests that not all active grains were captured by measuring the grinding wheel topography. This has already been addressed in section 3.1. In addition to the reasons already mentioned, the wear of the individual grains could also be a factor. This can result in the grains identified as active continuing to flatten during the process, causing additional grains to become active in the process.

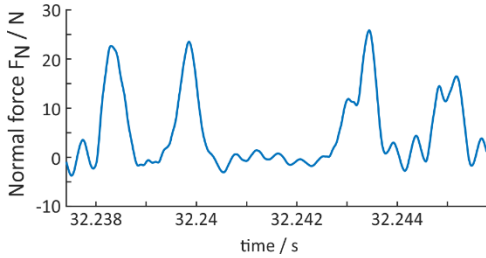


Figure 7. Averaged normal forces of all revolutions of the D851 grinding wheel machining with $v_c = 30$ m/s and $a_e = 1.5$ μ m

3.4. Process loads

As described, in several experiments the measured active grains matched the peaks in the force measurement. The process loads can be estimated for these selected experiments. The calculated process loads are shown in Figure 8. These are the average normal forces which have been calculated with the individual grain surfaces. As only two grain engagements could be registered in the force measurement for the parameter combination D301 and $v_c = 30$ m/s, the two closely spaced grain surfaces were considered together for the second force peak. Furthermore, the normal forces were considered and the tangential force was not taken into account, as the tangential forces did not show any significant peaks in the experiments and their magnitude was close to the noise of the force signal. A correlation between the process load and the speed cannot be identified. However, the grain size seems to have an influence on the process load. The individual grain positions of the D601 grinding wheel have higher process loads than the D301 grinding wheel.

Furthermore, no clear correlation can be determined by comparing the process loads with the surface roughness values S_q and S_{mr} . However, the data indicate that lower process loads (D301, $v_c = 30$ m/s) correlate with higher roughness S_q . Higher process loads occur in the experiments which resulted in lower roughness S_q . Furthermore, the S_{mr} value tends to indicate a ductile material removal at higher overall process loads. These observations are also consistent with the current state of knowledge, according to which high process loads lead to hydrostatic pressure and thus, promote ductile material removal.

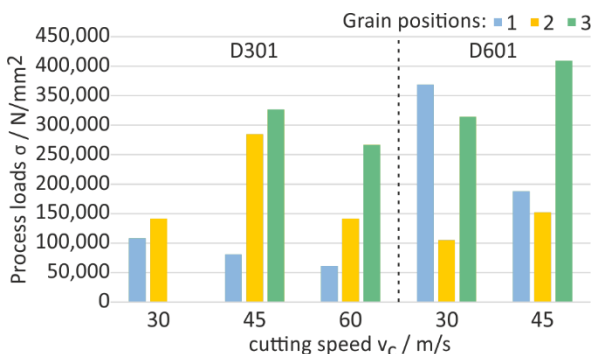


Figure 8. Exemplary process loads of the experiments for different grain positions

4. Summary and conclusions

It was shown that it is possible to measure the entire circumference of a grinding wheel and characterise the grains using optical measurement technology. This enables the calculation of the contact surfaces of the grains with the workpiece material. However, the results can be strongly influenced by the reflectivity and the clamping of the grinding wheel. Further potential for optimisation can therefore be identified here, which will be addressed in the future.

Furthermore, the individual revolutions of the grinding wheels during the process could be measured using a triggered high-resolution force measurement and a trigger. The peaks that occur during the revolutions and are repeated allow to draw conclusions about possible contacts between the grains of the grinding wheel and the workpiece. This makes it possible to assign the previously detected active grains to the forces enabling the process loads in the contact area to be estimated. This was also carried out exemplary in this work. However, an exact correlation between the process loads and the generated surface roughness cannot be determined.

Roughness S_q from 60 nm to 175 nm was achieved. A reduction in roughness with increasing cutting speed was observed for grinding wheels D301 and D851. This can be explained by the decreasing maximum chip thickness with increasing cutting speed.

Future work will concentrate on a more precise characterisation of the grinding wheel topography. Furthermore, investigations of the subsurface will take place in order to analyse a correlation between the calculated process loads and the characteristics of the subsurface.

Acknowledgements

This work is supported by the German Research Foundation (DFG) under Grant No. HE 3276/10-1, Project No. 435367659. The authors express their sincere gratitude to the DFG for their support.

References

- [1] Brinksmeier E, Mutlugünes Y, Klocke F, Aurich J C, Shore P, Ohmori H 2010 Ultra-Precision Grinding CIRP Ann. 59 P 652-671
- [2] Wang, J; Li, Y; Han, J; Xu, Q; Guo, Y Evaluating subsurface damage in optical glasses In Journal of the European Optical Society – Rapid Publications, 2011, 6/11001; S1-16
- [3] Brinksmeier E, Riemer O, Rickens K, Berger D 2016 Application potential of coarse-grained diamond grinding wheels for precision grinding of optical materials. Prod. Eng. 10 P 563–573
- [4] Malkin S 1989 Grinding Technology - Theory and Application of Machining with Abrasives, Ellis Horwood Ltd
- [5] Bifano T G, Dow T A, Scattergood R O 1991 Ductile-regime grinding: a new technology for machining brittle materials. Trans. o. t. ASME, Journal of Engineering for Industry 113 P 184–189
- [6] Adam, B., Riemer, O., Rickens, K., Heinzl, C. 2023. Precision grinding of BK7 glass with coarse-grained diamond grinding wheels. euspen – ICE 2023, Copenhagen, DK, P 501-502.
- [7] Adam, B., Riemer, O., Rickens, K., Heinzl, C. 2024. Precision plunge grinding with coarse-grained diamond grinding wheel. euspen – ICE 2024, Dublin, IE, P 281-284.